molecules

MDPI

Article

Thiazole–Chalcone Hybrids as Prospective Antitubercular and Antiproliferative Agents: Design, Synthesis, Biological, Molecular Docking Studies and In Silico ADME Evaluation

Ashok Babu Kasetti [1,2,*], Indrajeet Singhvi [3], Ravindra Nagasuri [4], Richie R. Bhandare [5,6,*] and Afzal B. Shaik [7,*]

1 Research Scholar, Faculty of Pharmacy, Pacific Academy of Higher Education and Research University, Pacific University, Udaipur 313003, India
2 Dr. Samuel George Institute of Pharmaceutical Sciences, Markapuram, Andhra Pradesh 523316, India
3 Faculty of Pharmacy, Pacific Academy of Higher Education and Research University, Pacific University, Udaipur 313003, India; indrajeetsinghvi@yahoo.com
4 A.M. Reddy Memorial College of Pharmacy, Narasaraopeta, Andhra Pradesh 523316, India; nravi1965@gmail.com
5 Department of Pharmaceutical Sciences, College of Pharmacy & Health Sciences, Ajman University, Ajman P.O. Box 346, United Arab Emirates
6 Center of Medical and Bio-Allied Health Sciences Research, Ajman University, Ajman P.O. Box 346, United Arab Emirates
7 Department of Pharmaceutical Chemistry, Vignan Pharmacy College, Vadlamudi, Guntur, Andhra Pradesh 522213, India
* Correspondence: soku4u@gmail.com (A.B.K.); r.bhandareh@ajman.ac.ae (R.R.B.); bashafoye@gmail.com (A.B.S.)

check for updates

Citation: Kasetti, A.B.; Singhvi, I.; Nagasuri, R.; Bhandare, R.R.; Shaik, A.B. Thiazole–Chalcone Hybrids as Prospective Antitubercular and Antiproliferative Agents: Design, Synthesis, Biological, Molecular Docking Studies and In Silico ADME Evaluation. *Molecules* **2021**, *26*, 2847. https://doi.org/10.3390/molecules26102847

Academic Editor: James Gauld

Received: 7 April 2021
Accepted: 8 May 2021
Published: 11 May 2021

Publisher's Note: MDPI stays neutral with regard to jurisdictional claims in published maps and institutional affiliations.

Abstract: Compounds bearing thiazole and chalcone pharmacophores have been reported to possess excellent antitubercular and anticancer activities. In view of this, we designed, synthesized and characterized a novel series of thiazole–chalcone hybrids (**1**–**20**) and further evaluated them for antitubercular and antiproliferative activities by employing standard protocols. Among the twenty compounds, chalcones **12** and **7**, containing 2,4-difluorophenyl and 2,4-dichlorophenyl groups, showed potential antitubercular activity higher than the standard pyrazinamide (MIC = 25.34 μM) with MICs of 2.43 and 4.41 μM, respectively. Chalcone **20** containing heteroaryl 2-thiazolyl moiety exhibited promising antiproliferative activity against the prostate cancer cell line (DU-145), higher than the standard methotrexate (IC_{50} = 11 ± 1 μM) with an IC_{50} value of 6.86 ± 1 μM. Furthermore, cytotoxicity studies of these compounds against normal human liver cell lines (L02) revealed that the target molecules were comparatively less selective against L02. Additional computational studies using AutoDock predicted the key binding interactions responsible for the activity and the SwissADME tool computed the in silico drug likeliness properties. The lead compounds generated through this study, create a way for the optimization and development of novel drugs against tuberculosis infections and prostate cancer.

Keywords: thiazole; chalcone; antiproliferative activity; antitubercular activity; cytotoxic activity; AutoDock; SwissADME

1. Introduction

Heterocyclic chemistry plays a pivotal role in the design and development of novel drug molecules as most drugs possess heterocyclic rings. In 2020, the US-FDA approved 24 small molecules and among them 22 molecules contained heterocyclic moieties [1]. This represents the impact of heterocyclic chemistry on the development of new therapies. Thiazole is one such five membered heterocyclic ring which constitutes an essential structural moiety of many marketed drugs. Many anticancer drugs like Dasatinib, Bleomycin, Epothiolone B, Tiazofuran possess a thiazole ring (Figure 1). Additionally, other drugs with a thiazole ring include Abafungin, Ravuconazole (antifungal agents),

Acinitrazole, Sulfathiazole (antibacterial agents), Micrococcin, Penicillins, third, fourth and fifth generation cephalosporins (antibacterial antibiotics), Nitazoxanide (antiprotozoal), Ritonavir (antiretroviral agent), Meloxicam (anti-inflammatory), Febuxostat (antigout agent), Famotidine, Nizatidine (antiulcer agents), Pramipexole (antidepressant), Chlormethiazole/Clomethiazole (sedative) and Thiamine (vitamin). Thiazole derivatives were extensively studied by organic and medicinal chemists for their diverse biological activities. The thiazole motif is important for altering the pharmacokinetic and pharmacodynamic properties of the drug molecules. It has exerted different roles in the lead identification and optimization including its use as a pharmacophore or spacer or a bioisosteric scaffold [2,3].

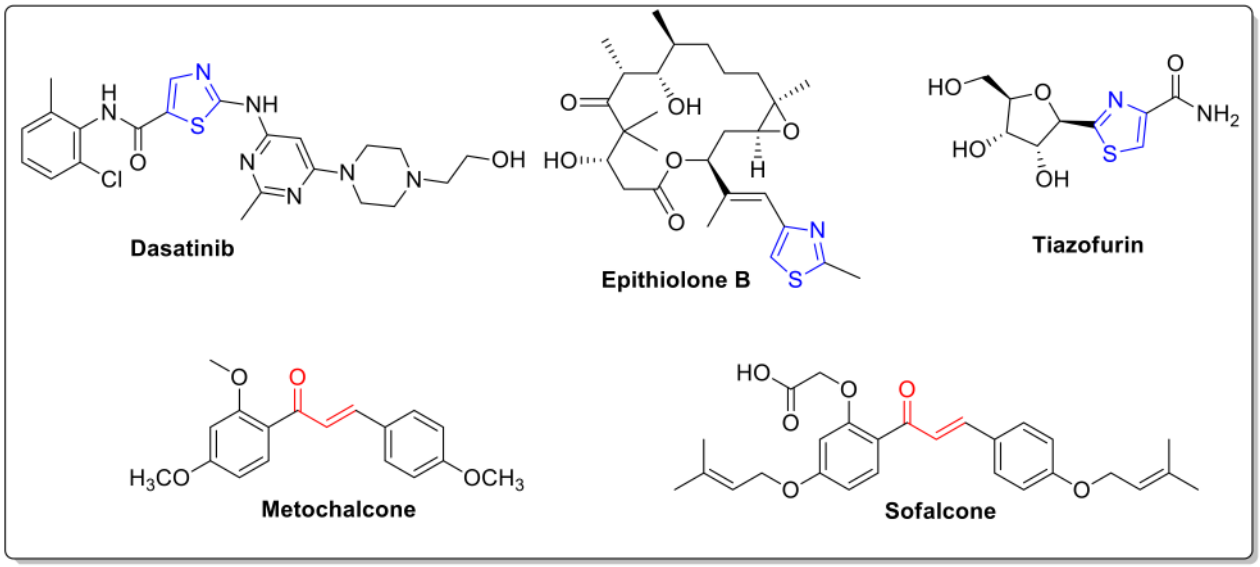

Figure 1. Structures of clinically approved thiazole and chalcone based drugs.

Chalcones are a group of natural open chain flavonoids with promising biological activities [4]. Chemically, chalcones are diarylpropenones (diaryl vinyl ketones) and their structure can be seen in clinically approved drugs including Metochalcone and Sofalcone (Figure 1). The vinyl ketone part of the chalcones is not only responsible for the biological activities of chalcones but is also useful as a key synthon for the preparation of different heterocyclic compounds of pharmacological interest [5]. Thiazole and chalcone derivatives possess a broad spectrum of bioactivities, including antitubercular [6–17], anticancer [18–32], antioxidant [33–38], antifungal [39–46] and antibacterial [47–55]. The nature of the substituents as well as the type of the aryl rings connected to the propenone bridge of chalcones governs the intensity of a given biological activity. The improved biological activity of the chalcones was observed with halogenated chalcones and the chalcones in which the aryl ring was replaced with heteroaryl rings. Interestingly, the incorporation of heterocyclic scaffolds and halogen substituted aryl rings improves the ADMET and pharmacodynamic properties of drugs and drug-like candidates [56]. The linking of two biologically active pharmacophoric groups is a practice followed by medicinal chemists for many years through molecular hybridization. Such combination approach will produce molecules with synergistic and higher bioactivity [57]. Additionally, the new structures that emerge due to molecular hybridization are typically rigid pharmacophores that are able to bind effectively to the target.

Thiazole–chalcone hybrids have been previously reported with promising antimicrobial [58], anticancer [24] and lipoxygenase (5-LOX) inhibitory [59] activities. In view of the above facts, we designed, synthesized and evaluated the antitubercular, antiproliferative and cytotoxic activities of 20 novel thiazole–chalcone hybrids (**1**–**20**) containing biologically active thiazole and chalcone pharmacophores in order to find novel lead molecules with improved biological activities (Figure 2).

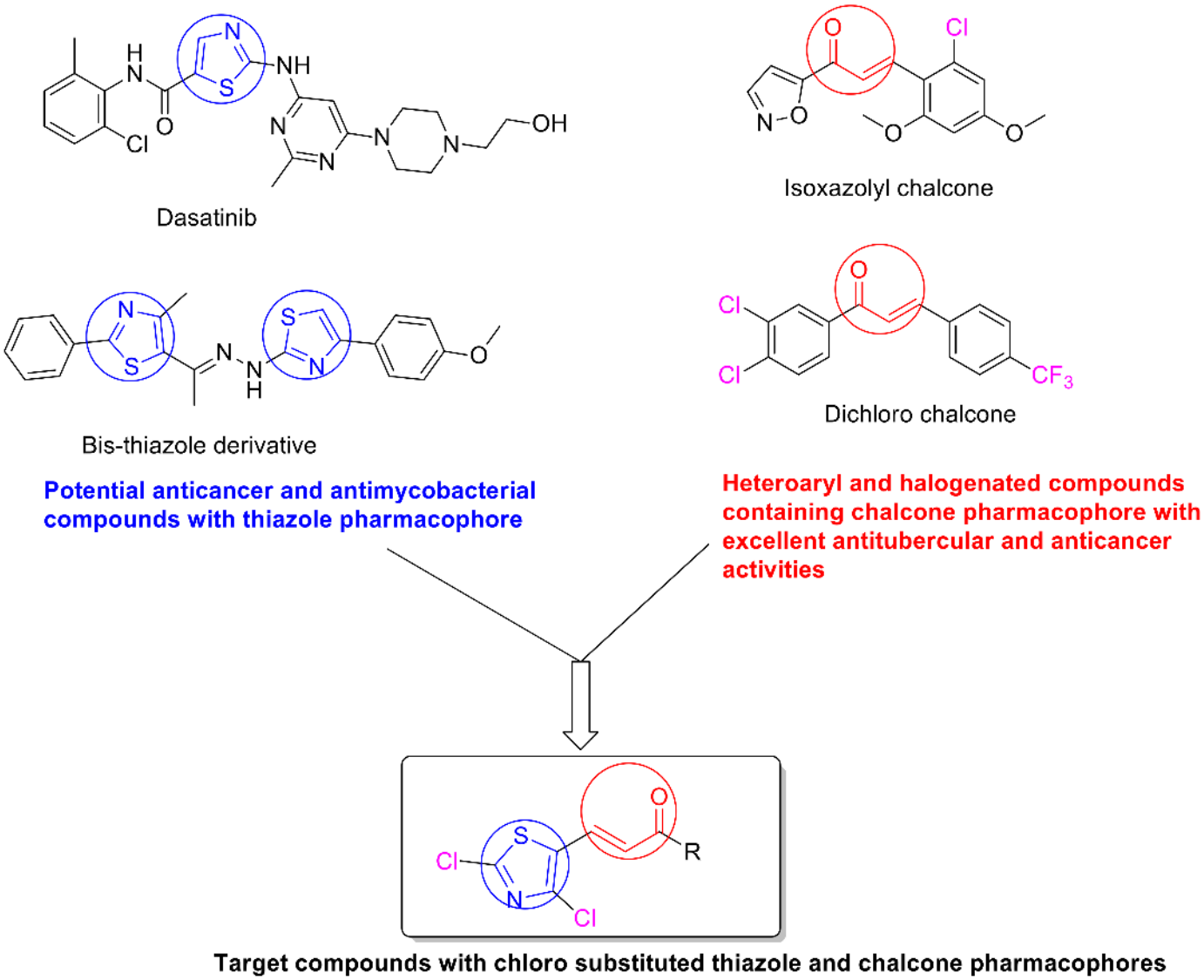

Figure 2. Design of thiazole–chalcone hybrids.

2. Results and Discussion

2.1. Chemistry

The target thiazole–chalcone hybrids were synthesized by the condensing of different substituted aromatic ketones with 2,4-dichlorothiazole-5-carboxaldehyde in the presence of a glacial acetic acid and hydrochloric acid mixture to isolate the compounds (**1**–**20**) in 75–91% yields. The synthesized hybrids were pale yellow-colored compounds with solubility in chloroform, methanol and DMSO. All the compounds were characterized by FT-IR, ^{1}H-NMR and mass spectrometry and the most potent compounds **7**, **12** and **20** were also characterized by ^{13}C-NMR spectroscopy. In the FT-IR spectrum, two diagnostic stretching absorption bands of C=O and HC=CH were seen around the wave numbers 1651–1698 cm^{-1} and 1506–1520 cm^{-1}, respectively. The ^{1}H-NMR spectra showed two doublet signals characteristic of the α- and β-protons of the propenone linkage resonating between the chemical shift values 7.27–7.89 ppm and 7.66–8.16 ppm. The coupling constant value J, for these doublets ranged between 15–17 Hz. These large coupling constant values confirmed the *trans* isomer of the olefinic bond present in the hybrids. ^{13}C-NMR spectrum of the compounds displayed the signals at δ 181.3–196.1 (C-1, C=O), 122.4–130.5 (C-2, O=C-CH=CH-), and 133.5–146.4 (C-3, O=C-CH=CH-) corresponding to the vinyl ketone portion of chalcone. The molecular ion peak in the mass spectrum further confirmed

the formation of chalcones. Additionally, all the compounds showed an isotopic M + 2 peak of one-third intensity to the molecular ion peak. The FT-IR, ^{1}H NMR, ^{13}C NMR and Mass Spectra for compounds can be found in the Supplementary Materials.

2.2. Biological Studies

All the compounds were evaluated for their antitubercular, antiproliferative and cytotoxicity activities by MABA and MTT assays and the results are portrayed in Tables 1 and 2, respectively. The target compounds (**1**–**20**) were classified into three series (Table 1): monosubstituted phenyl based chalcones (**1**–**3** and **9**–**11**), disubstituted phenyl based chalcones (**4**–**7** and **12**–**16**) and unsubstituted heteroaryl derivatives (bioisosteres of phenyl ring **17**–**20**). The electro withdrawing groups Cl or F were located at ortho (**1**, **9**), meta (**2**, **10**) and para (**3**, **11**) position whereas, in the disubstituted series, Cl or F were substituted at positions 2, 3; 2, 6; 2, 5; 2, 4; 3, 4 or 3, 5 on the phenyl ring.

Table 1. Antitubercular results of thiazole–chalcone hybrids (**1**–**20**).

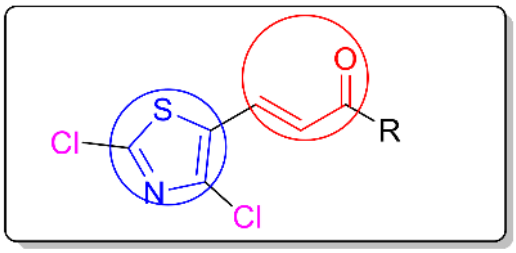

Entry	R	Mtb (H37Rv Strain) (MIC in μM) [a]
1	2-chlorophenyl	78.46 ± 1
2	3-chlorophenyl	313.87 ± 1
3	4-chlorophenyl	78.46 ± 1
4	2,3-dichlorophenyl	141.62 ± 2
5	2,6-dichlorophenyl	35.40 ± 2
6	2,5-dichlorophenyl	141.62 ± 1
7	2,4-dichlorophenyl	**4.41** ± 2
8	3,4-dichlorophenyl	141.62 ± 1
9	2-fluorophenyl	**20.68** ± 2
10	3-fluorophenyl	165.48 ± 1
11	4-fluorophenyl	**20.68** ± 1
12	2,4-difluorophenyl	**2.43** ± 1
13	2,5-difluorophenyl	39.04 ± 1
14	2,6-difluorophenyl	**9.74** ± 2
15	3,4-difluorophenyl	39.04 ± 1
16	3,5-difluorophenyl	156.18 ± 2
17	2-pyridinyl	350.70 ± 2
18	3-pyridinyl	701.40 ± 1
19	4-pyridinyl	350.70 ± 2
20	2-thiazolyl	343.45 ± 1
Pyrazinamide		25.34 ± 2

[a] MICs are mean of three independent experiments. Bold numerical values in third column represent compounds with highest activity.

2.2.1. Antitubercular Activity

The minimum inhibitory concentration (MIC) values for antitubercular activity ranged from 2.43 ± 2 to 701.40 ± 1 μM. Among the twenty compounds, five compounds **7**, **9**, **11**, **12** and **14** displayed more activity than the standard, pyrazinamide (MIC = 25.34 μM). In the monosubstituted series, the ortho (**1**, **9**) and para (**3**, **9**) positions were found to be beneficial for activity over the meta (**2**, **10**) position Among the monosubstituted chalcones **1**–**3**, **9**–**11**, the *ortho* and *para*-F substituted compounds showed 3.79-fold better activity over the Cl-containing compounds (MIC 20.68 ± 2 μM (**9**, **11**) vs. 78.46 ± 1 μM (**1**, **3**)). The MIC value was further improved when the phenyl ring was disubstituted with F over Cl

(MIC = 2.43 ± 1 μM (**12**), 4.41 ± 2 μM (**7**)). Compounds **12** and **7** bearing halogen atoms in both ortho and para positions, i.e., 2,4-difluorophenyl (MIC = 2.43 ± 1 μM) and 2,4-dichlorophenyl (MIC = 4.41 ± 2 μM) showed potencies 10.42 and 5.74 times more than the standard (MIC 25.34 ± 2 μM) whereas the monofluorinated compounds **9** and **11** bearing fluorine atoms at ortho and para positions, showed activity at MIC 20.68 μM which was 0.81 times greater than pyrazinamide (25.34 ± 2 μM). The chalcone **14** (MIC = 9.74 ± 2 μM) containing 2,6-difluorophenyl scaffold was 2.6-times more active than the standard. This suggests that the degree of electronegativity played a key role in modulating the physicochemical properties of the phenyl ring thereby influencing the antitubercular activity. Among the bioisosteres **17**–**20**, the activity ranged from 343.45 ± 1 to 701.40 ± 1 μM. No improvement in activity was observed over the standard pyrazinamide.

Table 2. Antiproliferative and cytotoxic activity results of thiazole–chalcone hybrids (**1**–**20**).

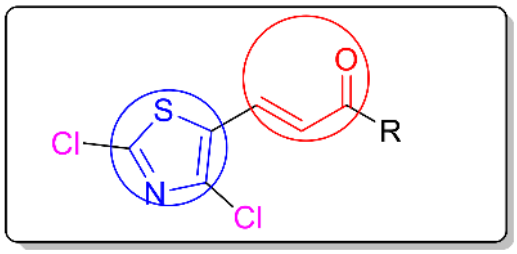

Entry	R	Prostate Cancer Cell Line (DU-145) (IC_{50} in μM) [b]	Normal Liver Cell Line (L02) (IC_{50} in μg/mL) [b]
1	2-chlorophenyl	100.43 ± 2	>70
2	3-chlorophenyl	1607.03 ± 2	>70
3	4-chlorophenyl	401.75 ± 1	>70
4	2,3-dichlorophenyl	181.28 ± 1	>70
5	2,6-dichlorophenyl	90.64 ± 1	>70
6	2,5-dichlorophenyl	2900.52 ± 2	>70
7	2,4-dichlorophenyl	181.28 ± 1	>70
8	3,4-dichlorophenyl	1450.26 ± 1	>70
9	2-fluorophenyl	52.95 ± 2	>70
10	3-fluorophenyl	847.28 ± 2	>70
11	4-fluorophenyl	423.64 ± 2	>70
12	2,4-difluorophenyl	99.95 ± 1	>70
13	2,5-difluorophenyl	3198.70 ± 2	>70
14	2,6-difluorophenyl	24.98 ± 2	>70
15	3,4-difluorophenyl	799.67 ± 1	>70
16	3,5-difluorophenyl	3198.70 ± 1	>70
17	2-pyridinyl	14.02 ± 1	>70
18	3-pyridinyl	28.05 ± 1	>70
19	4-pyridinyl	14.02 ± 1	>70
20	2-thiazolyl	**6.86 ± 1**	>70
Methotrexate		11 ± 1	>70

[b] Data presented as mean ± SD (n = 3). All the compounds and the standard dissolved in DMSO, diluted with culture medium containing 0.1% DMSO. The control cells were treated with culture medium containing 0.1% DMSO. Bold numerical value in third column represents compound with highest activity.

2.2.2. Antiproliferative and Cytotoxic Activities

With respect to antiproliferative activity, the $IC_{50's}$ ranged from 6.86 ± 1 to 2900 ± 2 μM. Methotrexate was used as standard, having IC_{50} of 11 ± 1 μM. The disubstituted phenyl based chalcones **5** and **14** fared better over the monosubstituted series (IC_{50s} 90.64 ± 1 μM (**5**), 24.98 ± 2 μM (**14**) vs. 100.43 ± 2 μM to 1607 ± 2 μM (**1**–**3**) and 423.64 ± 2 μM (**10**) to 847.28 ± 2 μM (**11**)). Surprisingly, ortho F phenyl substituted chalcone **9** showed IC_{50} of 52.95 ± 2 μM and this activity was further enhanced two-fold by having F on 2 and 6 position of the phenyl ring (IC_{50} 24.98 ± 2 μM **14**). Replacing the phenyl ring with bioisosteres proved to be beneficial for antiproliferative activity with IC_{50s} ranging from 6.86 ± 1 to 28.05 ± 1 μM (**17**–**20**). The five membered heterocycle 2-thiazolyl based chalcone

(**20**) showed the most potent activity with IC_{50} of 6.86 ± 1 µM and was 1.6-fold better than methotrexate. Compounds **17** and **19** containing 2-pyridinyl and 4-pyridinyl scaffolds exhibited IC_{50s} closer to standard. Overall, it can be seen that halogen substituted chalcones showed potential antitubercular activity whereas compounds having unsubstituted heteroaryl scaffold exhibited greater antiproliferative activity (Table 2). Additionally, the cytotoxic activity of the target compounds was found to have IC_{50} above 70 µg/mL on human normal cell lines (L02). It indicated that all the compounds were less selective against L02 than DU-145 and *Mycobacterium tuberculosis* H37Rv strain.

A summary of the structure–activity relationships (SAR) of novel thiazole–chalcone hybrids and the most potent antitubercular and antiproliferative compounds retrieved from this study are depicted in Figure 3.

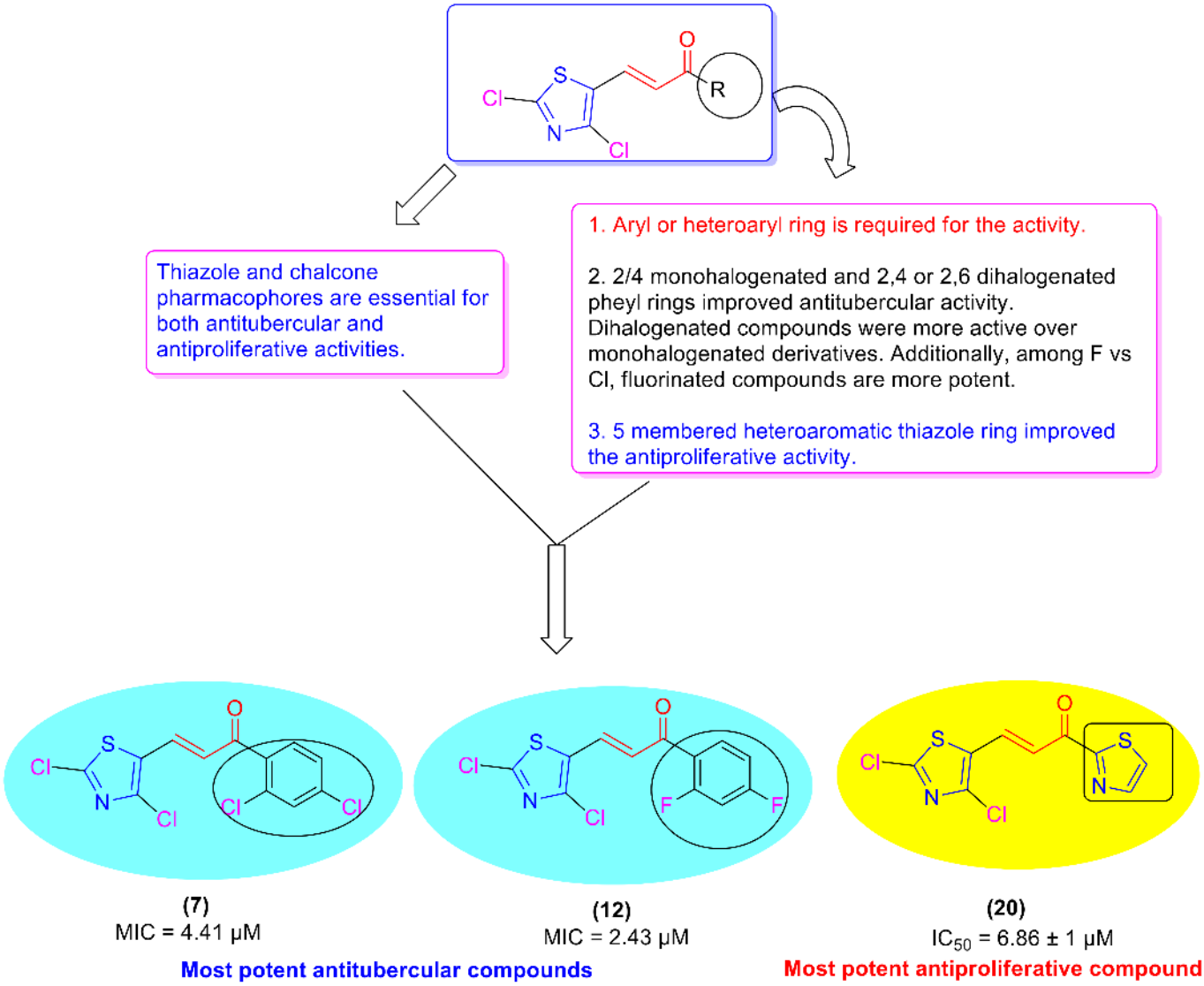

Figure 3. Structure–activity relationship (SAR) of thiazole–chalcone hybrids and structures of most potent antitubercular and antiproliferative compounds.

2.3. Computational Studies

2.3.1. Molecular Docking Studies

Molecular docking was carried out for selected compounds against the potential antitubercular and anticancer targets—Isocitrate Lyase and Topoisomerase IIa ATPase, respectively. The in silico antitubercular and anticancer activity results of selected ligands

against Isocitrate Lyase and Topoisomerase IIa ATPase were reported in terms of binding energy and ligand interactions with amino acid residues at active pocket of proteins. The in silico antitubercular results indicated that all compounds (**1**–**20**) showed strong binding affinity (ranges from −5.7 to −7.3, given in Table 3) towards the amino acid residues in active pocket Isocitrate Lyase protein through H-bond and hydrophobic interactions, compared to standard drug Pyrazinamide. The selected compounds having the electron withdrawing group substitution on the aromatic ring in place of the amine group may be the reason for the high affinity of these compounds compared to the standard drug pyrazinamide. Compounds **2** and **16** showed the highest binding affinity (−7.3).

Table 3. Docking scores of thiazole–chalcone hybrids against Isocitrate Lyase protein and Topoisomerase IIa ATPase.

Compound	Binding Affinity		Compound	Binding Affinity	
	1F8M	1ZXM		1F8M	1ZXM
1	−6.7	−8.1	**11**	−7	−7.8
2	−7.3	−8.1	**12**	−7.1	−8.2
3	−7	−7.7	**13**	−7.2	−8.4
4	−6.9	−7.9	**14**	−6.8	−8.2
5	−7.2	−7.9	**15**	−7.2	−8.2
6	−7.2	−8.1	**16**	−7.3	−8.3
7	−6.6	−8.1	**17**	−6.3	−7.6
8	−6.8	−8.1	**18**	−6.2	−7.7
9	−6.9	−8.1	**19**	−6.2	−7.7
10	−7.1	−8.1	**20**	−5.7	−9.3
Methotrexate	-	−9.5	**Pyrazinamide**	−5.4	-

Among all the compounds, compound **2** interacted with Trp320 amino acid residue through the H-bond and with Leu69, Cys314, Phe332, Ile346, Ala349, His352 amino acid residues through hydrophobic interaction. Similarly compounds **16**, **15**, **5**, **6**, **12** and other compounds also showed H-bond interactions with Trp320 and hydrophobic interaction but the standard drug pyrazinamide has H-bond interaction with Asp153, Arg228, Glu285, Asp108, Ser91, Leu348 amino acid residues and has hydrophobic interaction with Cys191, Thr347, His180 amino acid residues (Figures 4 and 5; Table 4). Moreover, the hydrophobic interactions between the functional groups of compounds and amino acid residues are more, compared to the hydrophobic interactions between the functional groups of standard drug pyrazinamide functional groups and amino acid residues of target protein. The compounds having the electron withdrawing group substituted on the aromatic ring in place of the amine group, and compounds having H-bond interaction with Trp320 amino acid residues and a greater number of hydrophobic interactions present between compounds and amino acid residues in the active site of the target protein may be the possible reason for the high affinity of the compounds when compared to standard drug pyrazinamide.

The in silico anticancer results of compounds (**1**–**20**) against Topoisomerase IIa ATPase revealed that none of the compounds showed a good binding affinity (ranging from −8.2 to −9.3 as given in Table 5) towards the amino acid residues when compared to the binding affinity of the standard drug Methotrexate (−9.5). The standard drug Methotrexate possessed H-bond interaction with Ile88, Asn120, Thr147, Asn150, Arg162, Gly164, Gly166 amino acid residues and hydrophobic interaction with Asn91, Ala92, Ile125, and Thr215 amino acid residues, given in Table 5 and depicted in Figures 6 and 7. However, compound **20**, having a 2-thiazole substitution, showed the least binding affinity (−9.3) among the all compounds (**1**–**20**), having H-bond interaction with Asn95, Ser149, Asn150, Arg168 and hydrophobic interaction with Arg98, Ala167 amino acid residues. Moreover, compounds with 2,5 dichlorophenyl substitution (**6**), 2, 5-difluoro phenyl substitution (**13**), 3,5-difluoro phenyl substitution (**16**), 2,4-difluoro phenyl substitution (**12**) had moderate binding affinity as -8.4, -8.3 and -8.2, respectively, towards amino acid residues like Asn95, Ser149, asn150,

Arg162, Asn163, Gly164, Ala167, Ays168, through the H-bond and amino acid residues like Arg98, Ala167, through hydrophobic interaction. Compounds with electron withdrawing groups at ortho and meta positions of phenyl substituent displayed moderate binding affinities, in addition to the H-bond between the compounds and Asn150 amino acid residue in the active site of target protein which may be highly essential for the good binding affinity of these compounds. The results also indicated that the compounds with 2-thiazoyl substitution had a similar binding affinity to that of the methotrexate.

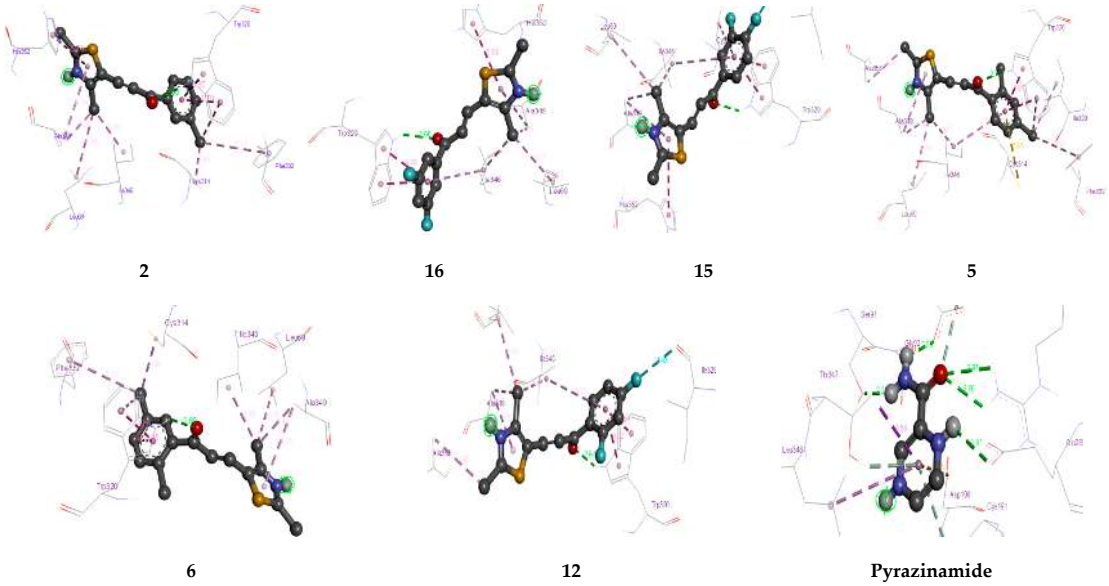

Figure 4. Three-dimensional interactions of selected compounds with Isocitrate Lyase protein amino acid residues.

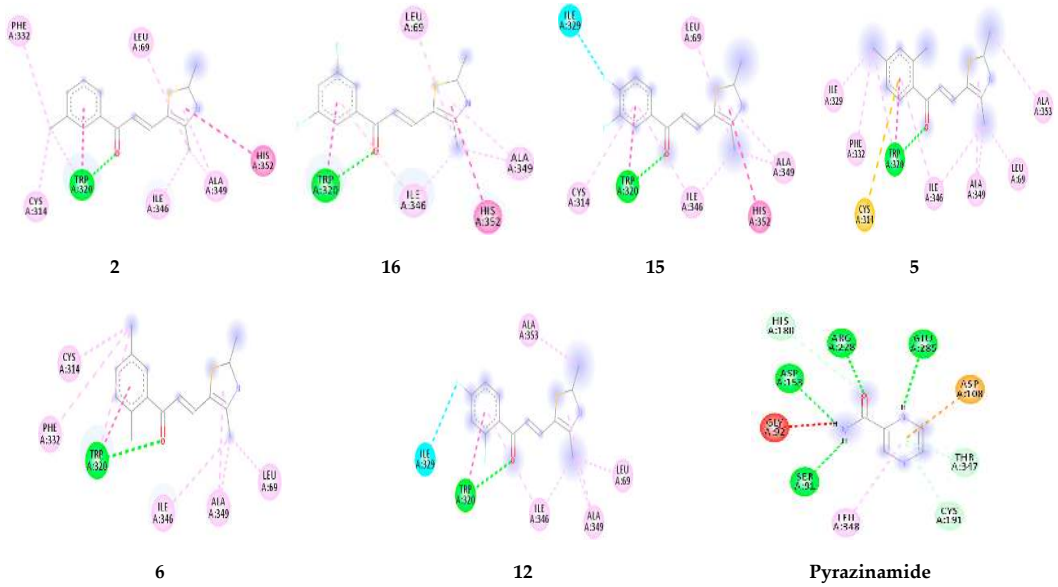

Figure 5. Two-dimensional interactions of selected compounds with Isocitrate Lyase protein amino acid residues.

Table 4. Molecular interactions of thiazole–chalcone hybrids with highest docking score against Isocitrate Lyase protein.

Compound	Docking Score	Amino Acids Interacted Through	
		H-Bond	Hydrophobic
2	−7.3	Trp320	Leu69, Cys314, Phe332, Ile346, Ala349, His352
16	−7.3	Trp320	Leu69, Ile346, Ala349, His352
15	−7.2	Trp320	Lue69, Ile329, Cys314, Ile346, Ala349, His352
5	−7.2	Trp320	Leu69, Ile329, Phe332, Ile346, Ala349, Ala353
6	−7.2	Trp320	Leu69, Lys315, Phe332, Ile346, Ala349
12	−7.1	Trp320	Leu69, Ile329, Ile346, Ala349, Ala353
Pyrazinamide	−5.4	Asp153, Arg228, Glu285, Asp108, Ser91, Leu348	Cys191, Thr347, His180

Table 5. Molecular interactions of thiazole–chalcone hybrids with highest docking score against Topoisomerase IIa ATPase.

Compound	Docking Score	Amino Acids Interacted Through	
		H-Bond	Hydrophobic
20	−9.3	Asn95, Ser149, Asn150, Lys168	Arg98, Ala167
6	−8.5	Asn95, Ser149, Asn150	Arg98, Ala167
13	−8.4	Asn95, Ser149, asn150, Arg162, Gly164	Arg98, Ala167
16	−8.3	Asn95, Ser149, Asn150, Arg162, Asn163, Gly163, Ala167, Ays168	Arg98
12	−8.2	Asn120, Phe142	Ile88, Ala92, Ile118, Ile141, Gly164, Ala167, Thr215, Ile217
Methotrexate	−9.5	Ile88, Asn120, Thr147, Asn150, Arg162, Gly164, Gly166	Asn91, Ala92, Ile125, Thr215

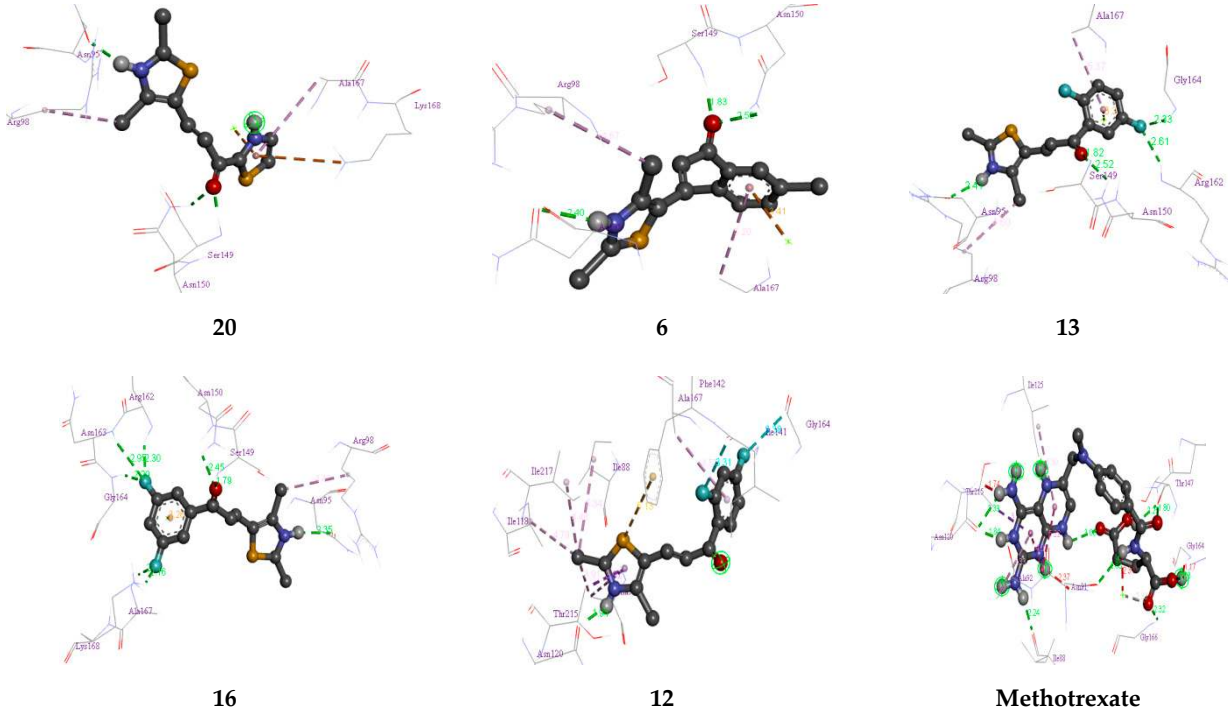

Figure 6. Three-dimensional interactions of selected compounds with Topoisomerase IIa ATPase protein amino acid residues.

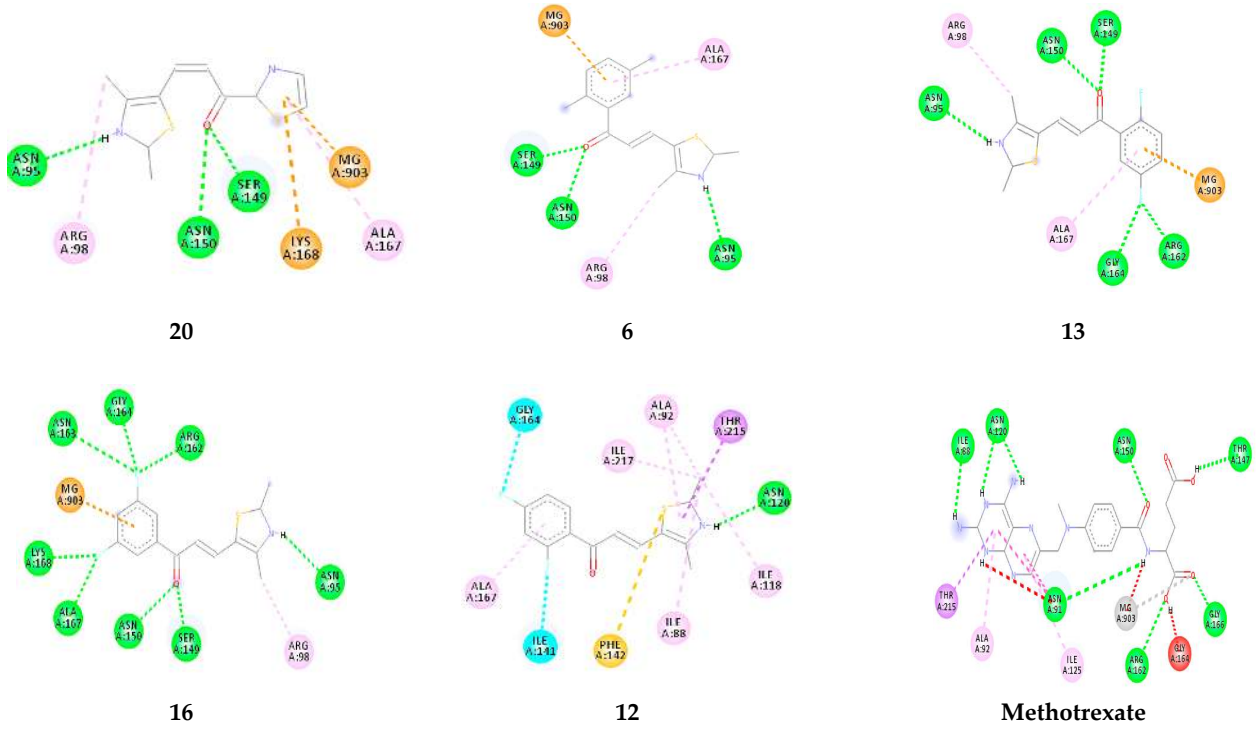

Figure 7. Two-dimensional interactions of selected compounds with Topoisomerase IIa ATPase protein amino acid residues.

2.3.2. In Silico Drug Likeliness Studies

Some selected compounds **7**, **14** and **20** which showed the best activity in antitubercular and antiproliferative activity were computed for certain properties using web-based SwissADME software (Table 6). It can be observed that they inhibited CYP2C19, but did not inhibit CYP2D6. However, they showed high GI absorption and passed the Lipinski Rule of five. Hence, these molecules have good drug-like properties and they can be taken as leads for further in vivo investigation.

Table 6. Computed properties using SWISSADME.

Compound #	GI Absorption	CYP2C19 Inhibitor	CYP2D6 Inhibitor	Lipinski #Violations
7	High	Yes	No	0
14	High	Yes	No	0
20	High	Yes	No	0

3. Materials and Methods

3.1. Chemistry

General protocol for the synthesis of thiazole–chalcone hybrids (**1**–**20**): Initially, 1 mmol of 2,4-dichlorothiazole-5-carboxaldehyde was dissolved in a mixture of glacial acetic acid (4 mL) and concentrated hydrochloric acid (2 mL) [60]. To the above solution, 1 mmol of corresponding aromatic ketone dissolved in 10 mL of ethanol was transferred and refluxed for 4–6 h. After completion of the reaction, the precipitate of the target compound was separated by filtration and washed thoroughly with cold water (50 mL × 2) and dried in a desiccator (Scheme 1). The crude precipitate was purified by column chromatography on silica gel using a mixture of hexane and ethyl acetate (2–25%).
(*E*)-1-(2-chlorophenyl)-3-(2,4-dichlorothiazol-5-yl)prop-2-en-1-one (**1**): Yield: 75%, m.p. 80 °C; FT-IR (KBr, cm^{-1}): 1656 (intense conjugated C=O band), 1506 (str, CH=CH, conjugated), 850.91, (C–Cl); ^{1}H-NMR spectrum (400 MHz, $CDCl_3$, ppm) δ (ppm): 7.28 (d, 1H, J = 16 Hz),

7.32–7.77 (m, 4H, Ar-H), 7.69 (d, 1H, *J* = 16 Hz); MS (*m*/*z*, %): 318.60 (M^+, 99.91) 320.60 (M + 2, 33.30).

(*E*)-1-(3-chlorophenyl)-3-(2,4-dichlorothiazol-5-yl)prop-2-en-1-one (**2**): Yield: 79%, m.p. 88 °C; FT-IR (KBr, cm^{-1}): 1651 (intense conjugated C=O band), 1508 (str, CH=CH, conjugated); ^{1}H-NMR spectrum (400 MHz, $CDCl_3$, ppm) δ (ppm): 7.27 (d, 1H, *J* = 16 Hz), 7.31–7.81 (m, 4H, Ar-H), 8.01 (d, 1H, *J* = 16 Hz); MS (*m*/*z*, %): 318.60 (M^+, 99.91) 320.60 (M + 2, 33.30).

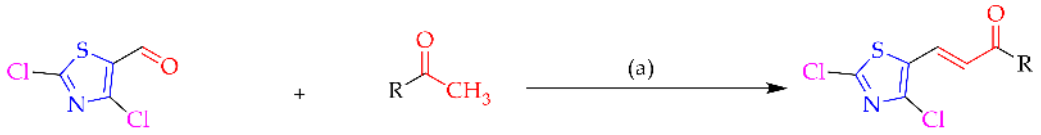

2,4-Dichlorothiazole-5-carboxaldehyde Aromatic ketones Thiazole-chalcone hybrids (**1-20**) (75-91% Yield)

R

1. 2-chlorophenyl; **2**. 3-chlorophenyl; **3**. 4-chlorophenyl; **4**. 2,3-dichlorophenyl; **5**. 2,6-dichlorophenyl; **6**. 2,5-dichlorophenyl; **7**. 2,4-dichlorophenyl; **8**. 3,4-dichlorophenyl; **9**. 2-fluorophenyl; **10**. 3-fluorophenyl; **11**. 4-fluorophenyl; **12**. 2,4-difluorophenyl; **13**. 2,5-difluorophenyl; **14**. 2,6-difluorophenyl; **15**. 3,4-difluorophenyl; **16**. 3,5-difluorophenyl; **17**. 2-pyridinyl; **18**. 3-pyridinyl; **19**. 4-pyridinyl; **20**. 2-thiazolyl

Scheme 1. Synthetic scheme for the preparation of novel thiazole–chalcone hybrids: (a) mixture of glacial acetic acid and hydrochloric acid, ethanol, refluxed for 4–6 h.

(*E*)-1-(4-chlorophenyl)-3-(2,4-dichlorothiazol-5-yl)prop-2-en-1-one (**3**): Yield: 84%, m.p. 104 °C; FT-IR (KBr, cm^{-1}): 1656 (intense conjugated C=O band), 1519 (str, CH=CH, conjugated); ^{1}H-NMR spectrum (400 MHz, $CDCl_3$, ppm) δ (ppm): 7.32 (d, 1H, *J* = 16 Hz), 7.36–7.85 (m, 4H, Ar-H), 8.06 (d, 1H, *J* = 16 Hz); MS (*m*/*z*, %): 318.60 (M^+, 99.91) 320.60 (M + 2, 33.30).

(*E*)-1-(2,3-dichlorophenyl)-3-(2,4-dichlorothiazol-5-yl)prop-2-en-1-one (**4**): Yield: 76%, m.p. 89 °C; FT-IR (KBr, cm^{-1}): 1682 (intense conjugated C=O band), 1514 (str, CH=CH, conjugated); ^{1}H-NMR spectrum (400 MHz, $CDCl_3$, ppm) δ (ppm): 7.36 (d, 1H, *J* = 15 Hz), 7.41–7.59 (m, 4H, Ar-H), 7.96 (d, 1H, *J* = 16 Hz); MS (*m*/*z*, %): 353.04 (M^+, 99.91) 355.04 (M + 2, 33.30).

(*E*)-1-(2,4-dichlorophenyl)-3-(2,4-dichlorothiazol-5-yl)prop-2-en-1-one (**5**): Yield: 88%, m.p. 101 °C; FT-IR (KBr, cm^{-1}): 1698 (intense conjugated C=O band), 1515 (str, CH=CH, conjugated); ^{1}H-NMR spectrum (400 MHz, $CDCl_3$, ppm) δ (ppm): 7.38 (d, 1H, *J* = 16 Hz), 7.48–7.67 (m, 4H, Ar-H), 8.16 (d, 1H, *J* = 16 Hz); MS (*m*/*z*, %): 353.04 (M^+, 99.91) 355.04 (M + 2, 33.30).

(*E*)-1-(2,5-dichlorophenyl)-3-(2,4-dichlorothiazol-5-yl)prop-2-en-1-one (**6**): Yield: 79%, m.p. 84 °C; FT-IR (KBr, cm^{-1}): 1677 (intense conjugated C=O band), 1509 (str, CH=CH, conjugated); ^{1}H-NMR spectrum (400 MHz, $CDCl_3$, ppm) δ (ppm): 7.41 (d, 1H, *J* = 16 Hz), 7.56–7.85 (m, 4H, Ar-H), 8.12 (d, 1H, *J* = 16 Hz); MS (*m*/*z*, %): 353.04 (M^+, 99.91) 355.04 (M + 2, 33.30).

(*E*)-1-(2,6-dichlorophenyl)-3-(2,4-dichlorothiazol-5-yl)prop-2-en-1-one (**7**): Yield: 83%, m.p. 112 °C; FT-IR (KBr, cm^{-1}): 1692 (intense conjugated C=O band), 1520 (str, CH=CH, conjugated); ^{1}H-NMR spectrum (400 MHz, $CDCl_3$, ppm) δ (ppm): 7.89 (d, 1H, *J* = 16 Hz), 7.54–7.75 (m, 4H, Ar-H), 8.09 (d, 1H, *J* = 16 Hz). ^{13}C-NMR spectrum (100 MHz, $CDCl_3$, ppm): 181.3 (C-1), 124.5 (C-2), 139.6 (C-3), 127.2, 131.1, 132.4, 134.5, 135.1, 135.9, 136.3, 146.3, 152.1 (Ar-C); MS (*m*/*z*, %): 353.04 (M^+, 99.91) 355.04 (M + 2, 33.30).

(*E*)-1-(3,4-dichlorophenyl)-3-(2,4-dichlorothiazol-5-yl)prop-2-en-1-one (**8**): Yield: 86%, m.p. 106 °C; FT-IR (KBr, cm^{-1}): 1675 (intense conjugated C=O band), 1516 (str, CH=CH, conjugated); ^{1}H-NMR spectrum (400 MHz, $CDCl_3$, ppm) δ (ppm): 7.66 (d, 1H, *J* = 16 Hz), 7.19–7.51 (m, 4H, Ar-H), 8.11 (d, 1H, *J* = 16 Hz); MS (*m*/*z*, %): 353.04 (M^+, 99.91) 355.04 (M + 2, 33.30).

(*E*)-1-(2-fluorophenyl)-3-(2,4-dichlorothiazol-5-yl)prop-2-en-1-one (**9**): Yield: 77%, m.p. 91 °C; FT-IR (KBr, cm^{-1}): 1679 (intense conjugated C=O band), 1508 (str, CH=CH, conjugated); ^{1}H-NMR spectrum (400 MHz, $CDCl_3$, ppm) δ (ppm): 7.45 (d, 1H, J = 16 Hz), 7.59–7.84 (m, 4H, Ar-H), 8.15 (d, 1H, J = 17 Hz); MS (m/z, %): 302.14 (M^+, 99.91) 304.14 (M + 2, 33.30).

(*E*)-1-(3-fluorophenyl)-3-(2,4-dichlorothiazol-5-yl)prop-2-en-1-one (**10**): Yield: 76%, m.p. 112 °C; FT-IR (KBr, cm^{-1}): 1688 (intense conjugated C=O band), 1516 (str, CH=CH, conjugated); ^{1}H-NMR spectrum (400 MHz, $CDCl_3$, ppm) δ (ppm): 7.33 (d, 1H, J = 16 Hz), 7.45–7.84 (m, 4H, Ar-H), 8.14 (d, 1H, J = 16 Hz); MS (m/z, %): 302.14 (M^+, 99.91) 304.14 (M + 2, 33.30).

(*E*)-1-(4-fluorophenyl)-3-(2,4-dichlorothiazol-5-yl)prop-2-en-1-one (**11**): Yield: 83%, m.p. 126 °C; FT-IR (KBr, cm^{-1}): 1681 (intense conjugated C=O band), 1518 (str, CH=CH, conjugated); ^{1}H-NMR spectrum (400 MHz, $CDCl_3$, ppm) δ (ppm): 7.42 (d, 1H, J = 16 Hz), 7.55–7.91 (m, 4H, Ar-H), 8.16 (d, 1H, J = 16 Hz); MS (m/z, %): 302.14 (M^+, 99.91) 304.14 (M + 2, 33.30).

(*E*)-1-(2,4-difluorophenyl)-3-(2,4-dichlorothiazol-5-yl)prop-2-en-1-one (**12**): Yield: 91%, m.p. 134 °C; FT-IR (KBr, cm^{-1}): 1656.38 (intense conjugated C=O band), 1497.38 (str, CH=CH, conjugated); ^{1}H-NMR spectrum (400 MHz, $CDCl_3$, ppm) δ (ppm): 7.51 (d, 1H, J = 16 Hz), 7.77–7.96 (m, 4H, Ar-H), 8.16 (d, 1H, J = 16 Hz). ^{13}C-NMR spectrum (100 MHz, $CDCl_3$, ppm): 196.1 (C-1), 130.5 (C-2), 146.4 (C-3), 128.6, 132.3, 133.8, 135.7, 136.4, 137.3, 138.5, 148.6, 154.6 (Ar-C); MS (m/z, %): 320.13 (M^+, 99.91) 322.13 (M + 2, 33.30).

(*E*)-1-(2,5-difluorophenyl)-3-(2,4-dichlorothiazol-5-yl)prop-2-en-1-one (**13**): Yield: 77%, m.p. 129 °C; FT-IR (KBr, cm^{-1}): 1674 (intense conjugated C=O band), 1512 (str, CH=CH, conjugated); ^{1}H-NMR spectrum (400 MHz, $CDCl_3$, ppm) δ (ppm): 7.55 (d, 1H, J = 16 Hz), 7.81–7.98 (m, 4H, Ar-H), 8.15 (d, 1H, J = 16 Hz); MS (m/z, %): 320.13 (M^+, 99.91) 322.13 (M + 2, 33.30).

(*E*)-1-(2,6-difluorophenyl)-3-(2,4-dichlorothiazol-5-yl)prop-2-en-1-one (**14**): Yield: 80%, m.p. 141 °C; FT-IR (KBr, cm^{-1}): 1666 (intense conjugated C=O band), 1511 (str, CH=CH, conjugated); ^{1}H-NMR spectrum (400 MHz, $CDCl_3$, ppm) δ (ppm): 7.69 (d, 1H, J = 16 Hz), 7.85–7.99 (m, 4H, Ar-H), 8.18 (d, 1H, J = 16 Hz); MS (m/z, %): 320.13 (M^+, 99.91) 322.13 (M + 2, 33.30).

(*E*)-1-(3,4-difluorophenyl)-3-(2,4-dichlorothiazol-5-yl)prop-2-en-1-one (**15**): Yield: 88%, m.p. 145 °C; FT-IR (KBr, cm^{-1}): 1675 (intense conjugated C=O band), 1516 (str, CH=CH, conjugated); ^{1}H-NMR spectrum (400 MHz, $CDCl_3$, ppm) δ (ppm): 7.33 (d, 1H, J = 16 Hz), 7.51–7.91 (m, 4H, Ar-H), 8.16 (d, 1H, J = 16 Hz); MS (m/z, %): 320.13 (M^+, 99.91) 322.13 (M + 2, 33.30).

(*E*)-1-(3,5-difluorophenyl)-3-(2,4-dichlorothiazol-5-yl)prop-2-en-1-one (**16**): Yield: 78%, m.p. 109 °C; FT-IR (KBr, cm^{-1}): 1688 (intense conjugated C=O band), 1519 (str, CH=CH, conjugated); ^{1}H-NMR spectrum (400 MHz, $CDCl_3$, ppm) δ (ppm): 7.36 (d, 1H, J = 16 Hz), 7.55–7.89 (m, 4H, Ar-H), 8.05 (d, 1H, J = 16 Hz); MS (m/z, %): 320.13 (M^+, 99.91) 322.13 (M + 2, 33.30).

(*E*)-3-(2,4-dichlorothiazol-5-yl)-1-(pyridin-2-yl)prop-2-en-1-one (**17**): Yield: 76%, m.p. 156 °C; FT-IR (KBr, cm^{-1}): 1658 (intense conjugated C=O band), 1509 (str, CH=CH, conjugated); ^{1}H-NMR spectrum (400 MHz, $CDCl_3$, ppm) δ (ppm): 7.32 (d, 1H, J = 16 Hz), 7.42–7.67 (m, 4H, Ar-H), 7.99 (d, 1H, J = 16 Hz); MS (m/z, %): 285.14 (M^+, 99.91) 287.14 (M + 2, 33.30).

(*E*)-3-(2,4-dichlorothiazol-5-yl)-1-(pyridin-3-yl)prop-2-en-1-one (**18**): Yield: 81%, m.p. 162 °C; FT-IR (KBr, cm^{-1}): 1662 (intense conjugated C=O band), 1506 (str, CH=CH, conjugated); ^{1}H-NMR spectrum (400 MHz, $CDCl_3$, ppm) δ (ppm): 7.38 (d, 1H, J = 16 Hz), 7.48–7.71 (m, 4H, Ar-H), 7.94 (d, 1H, J = 16 Hz); MS (m/z, %): 285.14 (M^+, 99.91) 287.14 (M + 2, 33.30).

(*E*)-3-(2,4-dichlorothiazol-5-yl)-1-(pyridin-4-yl)prop-2-en-1-one (**19**): Yield: 78%, m.p. 177 °C; FT-IR (KBr, cm^{-1}): 1660 (intense conjugated C=O band), 1509 (str, CH=CH, conjugated); ^{1}H-NMR spectrum (400 MHz, $CDCl_3$, ppm) δ (ppm): 7.34 (d, 1H, J = 16 Hz), 7.46–7.75 (m, 4H, Ar-H), 7.98 (d, 1H, J = 16 Hz); MS (m/z, %): 285.14 (M^+, 99.91) 287.14 (M + 2, 33.30).

(*E*)-3-(2,4-dichlorothiazol-5-yl)-1-(thiazol-2-yl)prop-2-en-1-one (**20**): Yield: 76%, m.p. 127 °C; FT-IR (KBr, cm^{-1}): 1657 (intense conjugated C=O band), 1507 (str, CH=CH, conjugated); ^{1}H-NMR spectrum (400 MHz, $CDCl_3$, ppm) δ (ppm): 7.36 (d, 1H, J = 16 Hz), 7.41–7.51 (m, 2H, Ar-H), 8.06 (d, 1H, J = 16 Hz). ^{13}C-NMR spectrum (100 MHz, $CDCl_3$, ppm): 190.6 (C-1), 122.4 (C-2), 133.5 (C-3), 127.8, 131.8, 135.9, 137.3, 136.2, 144.5, 151.2 (Ar-C); MS (m/z, %): 291.16 (M^+, 99.91) 293.16 (M + 2, 33.30).

3.2. Biological Studies

3.2.1. Antitubercular Activity

The antitubercular activity of all the target compounds (**1**–**20**) was tested against the *Mycobacterium tuberculosis H37Rv* strain. Pyrazinamide was used as the reference standard. In the present investigation, we employed the protocol described in the literature [61,62]. The icy culture of *Mycobacterium tuberculosis H37Rv* strain in Middlebrook 7H9 broth with the addition of 0.2% glycerol and 10% albumin-dextrose-catalase was defrosted and diluted in broth to 10^5 CFU mL^{-1} (colony forming unit/mL) dilutions. Separately, test compounds were dissolved in Dimethyl sulfoxide (DMSO) and later diluted with broth to achieve a concentration that was two-times the required concentration. Throughout this experiment, the final concentration of DMSO was 1.3% in the assay. Each test-tube used was then inoculated with 0.05 mL of standardized culture and then incubated for 21 days at 37 °C. The growth in the test-tubes was compared with the positive control, pyrazinamide and negative control, i.e., without inoculum and the drug. The minimum inhibitory concentration (MIC) of the individual target compound was determined by broth dilution assay. The MIC values were obtained in μg/mL and further these values were converted to micromoles (μM) considering the structural diversity of standard drug and the target compounds to draw a more meaningful conclusion.

3.2.2. Antiproliferative and Cytotoxic Activity

The in vitro antiproliferative and cytotoxicity of compounds **1**–**20** was evaluated by Mosmann's MTT (3-(4,5-dimethylthiazol-2-yl)-2,5-diphenyl tetrazolium bromide) assay method, as described in the literature [63–65] on prostate cancer cell lines (DU-145). In both the assays, the IC_{50} values of the tested compounds were compared with the positive control Methotrexate (Mtx). The reduction of the soluble MTT to blue-color formazan is the principle underlined in MTT assay and such change is chiefly due to the action of intracellular mitochondrial reductase in the living cells. The prostate cancer cell lines (DU-145), were cultured in Dulbecco's Modified Eagle Medium (DMEM**)** media at 37 °C and humidified at 5% CO_2 was used to culture prostate cancer cell lines (DU-145). The compounds (**1**–**20**) were initially dissolved in 0.1% DMSO to prepare their stock solutions. Later, the desired concentrations of the compounds were achieved by dissolving in sterile water. The cells were transferred on to 96-well plates at 100 μL total volume and with a density of 1×10^4 cells per well. The cells were permitted to adhere for a period of 24 h and then the assay medium was replaced with a fresh medium containing target compounds and incubated in DMEM with 10% fetal bovine serum (FBS) medium at 37 °C for an additional 48 h. Later, the medium was replaced with 90 μL of fresh DMEM without FBS. The above wells were treated with 10 μL of MTT reagent (5 mg/mL of stock solution in DMEM without FBS) and incubated for 3–4 h at 37 °C. The formed blue formazan crystals were dissolved in 200 μL of DMSO. The optical density was then determined at 570 nm using a micro plate reader. The assay was executed in triplicate for three independent experiments. The same trialing was also performed to confirm that the negative control-DMSO had no effect in the study. The results had good reproducibility between replicate wells with standard errors below 10%. The IC_{50} values measured in μg/mL for the antiproliferative were converted and expressed in μM. Additionally, all the compounds were also assessed for their cytotoxic activity on the normal human liver cell lines (L02) using the same protocol discussed above.

3.3. Computational Studies

3.3.1. Molecular Docking Studies

The X-ray crystal structures of Isocitrate Lyase (PDB ID: 1F8M) and Topoisomerase IIa ATPase (PDB ID: 1ZXM) were taken from protein data bank (rcsb.com/pdbdatabase (accessed on 7 April 2021)). Using PyMOL 2.3.4 the water molecules were removed and hydrogens were added as well as co-crystal ligands were extracted and saved in mol2 format. The mol2 format file of protein was loaded and then converted to pdbqt format using Autodock module Macromolecule tool in PyRx Virtual screening software 0.8 [66]. The 2D-structures of the target compounds (**1–20**) and that of the standard drugs-pyrazinamide and methotrexate were drawn in ChemDraw ultra 12.0 and saved as sdf file. The ligand files were subjected to energy minimization (force field-uff) through Open babel tool and then conformers for the selected ligands were generated through AutoDock pdbqt files in PyRx Virtual screening software 0.8. The docking was then performed through PyRx Virtual screening software 0.8 combined with AutoDock Vina, Open babel, Python shell tools. The prepared protein file and ligand files were selected through Vina module and the grid box was selected according to the previously reported amino acid residues by adjusting the x, y, z coordinates of grid box, then run the Vina. The results were analyzed by using DS visualizer software to visualize the interactions between ligands and amino acid residues of active site of protein (Kwofie et al., 2018).

3.3.2. In Silico Drug Likeliness Studies

To meet the requirements of the drug-likeliness, the properties of the most potent compounds **7**, **14** and **20** target compounds were evaluated for their in silico parameters including GI absorption, Lipinski rule of five as well as CYP2C19 CYP2D6 inhibition using SwissADME web (http://www.swissadme.ch/ (accessed on 24 March 2021)) [67].

4. Conclusions

In the present study we designed and synthesized 20 new thiazole–chalcone hybrids and tested all the compounds for antitubercular, antiproliferative and cytotoxic activities against *Mycobacterium tuberculosis* H37Rv strain, DU-145 (prostate cancer cell line) and human liver normal cells—LO2, respectively. We identified five potential antitubercular chalcones and one promising antiproliferative chalcone as they displayed better activity than the standard drugs. Among the five potent hybrids, the compounds **12** and **7** exhibited the strongest antitubercular activity with MIC values 2.43 and 4.41 μM correspondingly. The top most active antiproliferative hybrid **20** showed activity at IC_{50} value 6.86 ± 1 μM. All the compounds were subjected to molecular docking studies against antitubercular and anticancer drug targets and a good correlation was observed between the in vitro and docking results. Additionally, the calculated SwissADME properties of the most potent compounds **7**, **14** and **20** were in agreement with the required drug-like properties. All these results clearly confirm the usefulness of the active compounds for the furtherance of drug discovery and development against tuberculosis and prostate cancer.

Supplementary Materials: The following are available online: FT-IR, ^{1}H NMR, ^{13}C NMR and Mass Spectra for compounds.

Author Contributions: Conceptualization, A.B.K., I.S., R.N. and A.B.S.; methodology, A.B.K., I.S. and NR.; software, A.B.K., I.S., R.N., R.R.B. and A.B.S.; validation, A.B.K., I.S., R.N., R.R.B. and A.B.S.; formal analysis, A.B.K., I.S., R.N., R.R.B. and A.B.S.; investigation, A.B.K., I.S. and R.N.; resources, A.B.K., I.S. and R.N.; data curation, A.B.K., I.S. and R.N.; writing—original draft preparation, A.B.K., I.S., R.N., R.R.B. and A.B.S.; writing—review and editing, A.B.K., I.S., R.N., R.R.B. and A.B.S.; visualization, A.B.K., I.S., R.N., R.R.B. and A.B.S.; supervision, I.S. and R.N.; project administration, A.B.K., I.S. and R.N.; funding acquisition, A.B.K. and I.S. All authors have read and agreed to the published version of the manuscript.

Funding: This research received no external funding. However, the manuscript received partial funding from Ajman University, United Arab Emirates to cover the article processing charges.

Acknowledgments: K.A.B. and I.S. would like to thank Samuel George Institute of Pharmaceutical Sciences, Andhra Pradesh, India for providing the lab facilities and chemicals for this work. R.R.B. and A.B.S. would like to thank the Dean's office of College of Pharmacy and Health Sciences, Ajman University, UAE and Vignan Pharmacy College, Vadlamudi, Andhra Pradesh, India for their support in the preparation of this manuscript.

Conflicts of Interest: The authors declare no conflict of interest.

Sample Availability: Samples of the compounds are available from the authors.

References

1. Novel Drug Approvals for 2020. Available online: https://www.fda.gov/drugs/new-drugs-fda-cders-new-molecular-entities-and-new-therapeutic-biological-products/novel-drug-approvals-2020 (accessed on 20 December 2020).
2. Ayati, A.; Emami, S.; Asadipour, A.; Shafiee, A.; Foroumadi, A. Recent applications of 1, 3-thiazole core structure in the identification of new lead compounds and drug discovery. *Eur. J. Med. Chem.* **2015**, *5*, 699–718. [CrossRef] [PubMed]
3. Chhabria, T.M.; Patel, S.; Modi, P.; Brahmkshatriya, S.P. Thiazole: A review on chemistry, synthesis and therapeutic importance of its derivatives. *Curr. Top. Med. Chem.* **2016**, *16*, 2841–2862. [CrossRef] [PubMed]
4. Chunlin, Z.; Wen, Z.; Chunquan, S.; Wannian, Z.; Chengguo, X.; Zhenyuan, M. Chalcone: A Privileged Structure in Medicinal Chemistry. *Chem. Rev.* **2017**, *117*, 7762–7810. [CrossRef]
5. Yazdan, K.S.; Sagar, G.V.; Shaik, B.A. Biological and synthetic potentiality of chalcones: A review. *J. Chem. Pharm. Res.* **2015**, *7*, 829–842.
6. Abhale, Y.K.; Shinde, A.; Deshmukh, K.K.; Nawale, L.; Sarkar, D.; Mhaske, P.C. Synthesis, antitubercular and antimicrobial potential of some new thiazole substituted thiosemicarbazide derivatives. *Med. Chem. Res.* **2017**, *26*, 2557–2567. [CrossRef]
7. Dhumal, S.T.; Deshmukh, A.R.; Bhosle, M.R.; Khedkar, V.M.; Nawale, L.U.; Sarkar, D.; Mane, R.A. Synthesis and antitubercular activity of new 1, 3, 4-oxadiazoles bearing pyridyl and thiazolyl scaffolds. *Bioorg. Med. Chem. Lett.* **2016**, *26*, 3646–3651. [CrossRef]
8. Güzeldemirci, N.U.; Karaman, B.; Küçükbasmaci, Ö. Antibacterial, antitubercular and antiviral activity evaluations of some arylidenehydrazide derivatives bearing imidazo [2,1-b] thiazole moiety. *Turk. J. Pharm. Sci.* **2017**, *14*, 157. [CrossRef]
9. Yan, M.; Xu, L.; Wang, Y.; Wan, J.; Liu, T.; Liu, W.; Wan, Y.; Zhang, B.; Wang, R.; Li, Q. Opportunities and challenges of using five-membered ring compounds as promising antitubercular agents. *Drug. Dev. Res.* **2020**, *81*, 402–418. [CrossRef]
10. Kryshchyshyn, A.; Roman, O.; Lozynskyi, A.; Lesyk, R. Thiopyrano [2,3-*d*]Thiazoles as New Efficient Scaffolds in Medicinal Chemistry. *Sci. Pharm.* **2018**, *86*, 26. [CrossRef]
11. Gundlewad, G.B.; Patil, B.R. Synthesis and Evaluation of Some Novel 2-Amino-4-Aryl Thiazoles for Antitubercular Activity. *J. Het. Chem.* **2018**, *55*, 769–774. [CrossRef]
12. Shaik, A.B.; Bhandare, R.R.; Nissankararao, S.; Edis, Z.; Tangirala, N.R.; Shahanaaz, S.; Rahman, M.M. Design, facile synthesis and characterization of dichloro substituted chalcones and dihydropyrazole derivatives for their antifungal, antitubercular and antiproliferative activities. *Molecules* **2020**, *25*, 3188. [CrossRef]
13. Pola, S.; Banoth, K.K.; Sankaranarayanan, M.; Ummani, R.; Garlapati, A. Design, synthesis, in silico studies, and evaluation of novel chalcones and their pyrazoline derivatives for antibacterial and antitubercular activities. *Med. Chem. Res.* **2020**, *29*, 1819–1835. [CrossRef]
14. Burmaoglu, S.; Algul, O.; Gobek, A.; Aktas, A.D.; Ulger, M.; Erturk, B.G.; Kaplan, E.; Dogen, A.; Aslan, G. Design of potent fluoro-substituted chalcones as antimicrobial agents. *J. Enzyme. Inhib. Med. Chem.* **2017**, *32*, 490–495. [CrossRef]
15. Borcea, A.-M.; Ionuț, I.; Crișan, O.; Oniga, O. An Overview of the Synthesis and Antimicrobial, Antiprotozoal, and Antitumor Activity of Thiazole and Bisthiazole Derivatives. *Molecules* **2021**, *26*, 624. [CrossRef]
16. Kishor, P.; Ramana, K.V.; Shaik, A.B. Antitubercular evaluation of isoxazolyl chalcones. *Res. J. Pharm. Biol. Chem. Sci.* **2017**, *8*, 730–735.
17. Lokesh, B.V.; Prasad, Y.R.; Shaik, A.B. Synthesis and biological activity of novel 2, 5-dichloro-3-acetylthiophene chalcone derivatives. *Ind. J. Pharm. Educ. Res.* **2017**, *51*, 679–690. [CrossRef]
18. De Santana, T.I.; De Oliveira, B.M.; De Moraes, G.P.A.; Da Cruz, A.C.; Da Silva, T.G.; Leite, A.C. Synthesis, anticancer activity and mechanism of action of new thiazole derivatives. *Eur. J. Med. Chem.* **2018**, *20*, 874–886. [CrossRef]
19. Gomha, S.M.; Edrees, M.M.; Altalbawy, F.M.A. Synthesis and Characterization of Some New *Bis*-Pyrazolyl-Thiazoles Incorporating the Thiophene Moiety as Potent Anti-Tumor Agents. *Int. J. Mol. Sci.* **2016**, *17*, 1499. [CrossRef]
20. Takac, P.; Kello, M.; Vilkova, M.; Vaskova, J.; Michalkova, R.; Mojzisova, G.; Mojzis, J. Antiproliferative Effect of Acridine Chalcone Is Mediated by Induction of Oxidative Stress. *Biomolecules* **2020**, *10*, 345. [CrossRef]
21. Gomha, S.M.; Ahmed, S.A.; Abdelhamid, A.O. Synthesis and Cytotoxicity Evaluation of Some Novel Thiazoles, Thiadiazoles, and Pyrido [2,3-*d*][1,2,4]triazolo[4,3-*a*]pyrimidin-5(1*H*)-ones Incorporating Triazole Moiety. *Molecules* **2015**, *20*, 1357–1376. [CrossRef]
22. Patel, S.; Patle, R.; Parameswaran, P.; Jain, A.; Shard, A. Design, computational studies, synthesis and biological evaluation of thiazole-based molecules as anticancer agents. *Eur. J. Pharm. Sci.* **2019**, *134*, 20–30. [CrossRef]
23. Abu-Melha, S.; Edrees, M.M.; Salem, H.H.; Kheder, N.A.; Gomha, S.M.; Abdelaziz, M.R. Synthesis and biological evaluation of some novel thiazole-based heterocycles as potential anticancer and antimicrobial agents. *Molecules* **2019**, *24*, 539. [CrossRef]

24. Farghaly, T.A.; Masaret, G.S.; Muhammad, Z.A.; Harras, M.F. Discovery of thiazole-based-chalcones and 4-hetarylthiazoles as potent anticancer agents: Synthesis, docking study and anticancer activity. *Bioorg. Chem.* **2020**, *98*, 103761. [CrossRef]
25. Altıntop, M.D.; Sever, B.; Akalın, Ç.G.; Özdemir, A. Design, synthesis, and evaluation of a new series of thiazole-based anticancer agents as potent Akt inhibitors. *Molecules* **2018**, *23*, 1318. [CrossRef]
26. Spanò, V.; Attanzio, A.; Cascioferro, S.; Carbone, A.; Montalbano, A.; Barraja, P.; Tesoriere, L.; Cirrincione, G.; Diana, P.; Parrino, B. Synthesis and Antitumor Activity of New Thiazole Nortopsentin Analogs. *Mar. Drugs* **2016**, *14*, 226. [CrossRef]
27. Shaik, A.B.; Bhandare, R.R.; Nissankararao, S.; Lokesh, B.V.; Shahanaaz, S.; Rahman, M.M. Synthesis, and biological screening of chloropyrazine conjugated benzothiazepine derivatives as potential antimicrobial, antitubercular and cytotoxic agents. *Arab. J. Chem.* **2021**, *14*, 102915. [CrossRef]
28. Wang, Y.; Zhang, W.; Dong, J.; Gao, J. Design, synthesis and bioactivity evaluation of coumarin-chalcone hybrids as potential anticancer agents. *Bioorg. Chem.* **2020**, *95*, 103530. [CrossRef]
29. Shaik, A.; Bhandare, R.R.; Palleapati, K.; Nissankararao, S.; Kancharlapalli, V.; Shaik, S. Antimicrobial, Antioxidant, and Anticancer Activities of Some Novel Isoxazole Ring Containing Chalcone and Dihydropyrazole Derivatives. *Molecules* **2020**, *25*, 1047. [CrossRef]
30. Madhavi, S.; Sreenivasulu, R.; Yazala, J.P.; Raju, R.R. Synthesis of chalcone incorporated quinazoline derivatives as anticancer agents. *Saudi. Pharml. J.* **2017**, *25*, 275–279. [CrossRef]
31. Rashdan, H.R.M.; Abdelmonsef, A.H.; Shehadi, I.A.; Gomha, S.M.; Soliman, A.M.M.; Mahmoud, H.K. Synthesis, Molecular Docking Screening and Anti-Proliferative Potency Evaluation of Some New Imidazo[2,1-b]Thiazole Linked Thiadiazole Conjugates. *Molecules* **2020**, *25*, 4997. [CrossRef]
32. Madhavi, S.; Sreenivasulu, R.; Yousuf, A.M.; Jawed, A.M.; Ramesh, R.R. Synthesis, biological evaluation and molecular docking studies of pyridine incorporated chalcone derivatives as anticancer agents. *Lett. Org. Chem.* **2016**, *13*, 682–692. [CrossRef]
33. Djukic, M.; Fesatidou, M.; Xenikakis, I.; Geronikaki, A.; Angelova, V.T.; Savic, V.; Pasic, M.; Krilovic, B.; Djukic, D.; Gobeljic, B.; et al. In vitro antioxidant activity of thiazolidinone derivatives of 1, 3-thiazole and 1, 3, 4-thiadiazole. *Chem.-Biol. Interact.* **2018**, *286*, 119–131. [CrossRef] [PubMed]
34. Adole, V.A.; More, R.A.; Jagdale, B.S.; Pawar, T.B.; Chobe, S.S. Efficient synthesis, antibacterial, antifungal, antioxidant and cytotoxicity study of 2-(2-hydrazineyl) thiazole derivatives. *ChemistrySelect* **2020**, *5*, 2778–2786. [CrossRef]
35. Nastasă, C.; Tiperciuc, B.; Duma, M.; Benedec, D.; Oniga, O. New hydrazones bearing thiazole scaffold: Synthesis, characterization, antimicrobial, and antioxidant investigation. *Molecules* **2015**, *20*, 17325–17338. [CrossRef]
36. Polo, E.; Ibarra-Arellano, N.; Prent-Peñaloza, L.; Morales-Bayuelo, A.; Henao, J.; Galdámez, A.; Gutiérrez, M. Ultrasound-assisted synthesis of novel chalcone, heterochalcone and bis-chalcone derivatives and the evaluation of their antioxidant properties and as acetylcholinesterase inhibitors. *Bioorg. Chem.* **2019**, *90*, 103034. [CrossRef]
37. Wang, J.; Huang, L.; Cheng, C.; Li, G.; Xie, J.; Shen, M.; Chen, Q.; Li, W.; He, W.; Qiu, P.; et al. Design, synthesis and biological evaluation of chalcone analogues with novel dual antioxidant mechanisms as potential anti-ischemic stroke agents. *Acta Pharm. Sin. B* **2019**, *9*, 335–350. [CrossRef]
38. Al Zahrani, N.A.; El-Shishtawy, R.M.; Elaasser, M.M.; Asiri, A.M. Synthesis of Novel Chalcone-Based Phenothiazine Derivatives as Antioxidant and Anticancer Agents. *Molecules* **2020**, *25*, 4566. [CrossRef]
39. Asiri, A.M.; Khan, S.A. Synthesis and Anti-Bacterial Activities of a Bis-Chalcone Derived from Thiophene and Its Bis-Cyclized Products. *Molecules* **2011**, *16*, 523–531. [CrossRef]
40. Kadhim, A.J.; Mohammed, J.H.; Aljamali, N.M. Thiazole Amide Derivatives (Synthesis, Spectral Investigation, Chemical Properties, Antifungal Assay). *NeuroQuantology* **2020**, *18*, 16. [CrossRef]
41. Kucerova-Chlupacova, M.; Vyskovska-Tyllova, V.; Richterova-Finkova, L.; Kunes, J.; Buchta, V.; Vejsova, M.; Paterova, P.; Semelkova, L.; Jandourek, O.; Opletalova, V. Novel Halogenated Pyrazine-Based Chalcones as Potential Antimicrobial Drugs. *Molecules* **2016**, *21*, 1421. [CrossRef]
42. Shaik, A.B.; Yejella, R.P.; Shaik, S. Synthesis, Antimicrobial, and Computational Evaluation of Novel Isobutylchalcones as Antimicrobial Agents. *Int. J. Med. Chem.* **2017**, *2017*, 6873924. [CrossRef]
43. Singh, G.; Arora, A.; Kalra, P.; Maurya, I.K.; Ruizc, C.E.; Estebanc, M.A.; Sinha, S.; Goyal, K.; Sehgal, R. A strategic approach to the synthesis of ferrocene appended chalcone linked triazole allied organosilatranes: Antibacterial, antifungal, antiparasitic and antioxidant studies. *Bioorg. Med. Chem.* **2019**, *27*, 188–195. [CrossRef]
44. Shaik, A.B.; Lohitha, S.V.; Puttagunta, S.B.; Shaik, A.; Supraja, K.; Sai, H.K. Synthesis and screening of novel lipophilic diarylpropeones as prospective antitubercular, antibacterial and antifungal agents. *Biointerface Res. Appl. Chem.* **2019**, *9*, 3912–3918. [CrossRef]
45. Mellado, M.; Espinoza, L.; Madrid, A.; Mella, J.; Chávez-Weisser, E.; Diaz, K.; Cuellar, M. Design, synthesis, antifungal activity, and structure–activity relationship studies of chalcones and hybrid dihydrochromane–chalcones. *Mol. Divers.* **2019**, *3*, 1–3. [CrossRef]
46. Lagu, S.B.; Rajendra, P.Y.; Srinath, N.; Afzal, B.S. Synthesis. antibacterial, antifungal antitubercular activities and molecular docking studies of nitrophenyl derivatives. *Int. J. Life Sci. Pharma Res.* **2019**, *9*, 54–64. [CrossRef]
47. Sun, N.; Lu, Y.J.; Chan, F.Y.; Du, R.L.; Zheng, Y.Y.; Zhang, K.; So, L.Y.; Abagyan, R.; Zhuo, C.; Leung, Y.C.; et al. A thiazole orange derivative targeting the bacterial protein FtsZ shows potent antibacterial activity. *Front. Microbiol.* **2017**, *8*, 855. [CrossRef]

48. Abdel-Latif, E.; Almatari, A.S.; Abd-ElGhani, G.E. Synthesis and Antibacterial Evaluation of Some New Thiazole-Based Polyheterocyclic Ring Systems. *J. Heterocycl. Chem.* **2019**, *56*, 1978–1985. [CrossRef]
49. Vegesna, S.R.; Prasad, Y.R.; Afzal, B.S. Antimicrobial evaluation of some novel pyrazine based chalcones. *Int. J. Adv. Pharm. Sci.* **2017**, *8*, 11–18.
50. Özdemir, A.; Altıntop, M.D.; Sever, B.; Gençer, H.K.; Kapkaç, H.A.; Atlı, Ö.; Baysal, M. A New Series of Pyrrole-Based Chalcones: Synthesis and Evaluation of Antimicrobial Activity, Cytotoxicity, and Genotoxicity. *Molecules* **2017**, *22*, 2112. [CrossRef]
51. Tang, X.; Su, S.; Chen, M.; He, J.; Xia, R.; Guo, T.; Chen, Y.; Zhang, C.; Wang, J.; Xue, W. Novel chalcone derivatives containing a 1, 2, 4-triazine moiety: Design, synthesis, antibacterial and antiviral activities. *RSC. Adv.* **2019**, *9*, 6011–6020. [CrossRef]
52. Lagu, S.B.; Yejella, R.P.; Bhandare, R.R.; Shaik, A.B. Design, Synthesis, and Antibacterial and Antifungal Activities of Novel Trifluoromethyl and Trifluoromethoxy Substituted Chalcone Derivatives. *Pharmaceuticals* **2020**, *13*, 375. [CrossRef] [PubMed]
53. Reddy, P.V.; Hridhay, M.; Nikhil, K.; Khan, S.; Jha, P.N.; Shah, K.; Kumar, D. Synthesis and investigations into the anticancer and antibacterial activity studies of β-carboline chalcones and their bromide salts. *Bioorg. Med. Chem. Lett.* **2018**, *28*, 1278–1282. [CrossRef]
54. Khan, S.A.; Asiri, A.M. Green synthesis, characterization and biological evaluation of novel chalcones as antibacterial agents. *Arab. J. Chem.* **2017**, *10*, S2890-5. [CrossRef]
55. Zhang, M.; Prior, A.M.; Maddox, M.M.; Shen, W.J.; Hevener, K.E.; Bruhn, D.F.; Lee, R.B.; Singh, A.P.; Reinicke, J.; Simmons, C.J.; et al. Pharmacophore modeling, synthesis, and antibacterial evaluation of chalcones and derivatives. *ACS. Omega.* **2018**, *3*, 18343–18360. [CrossRef]
56. Gomtsyan, A. Heterocycles in drugs and drug discovery. *Chem. Heterocycl. Com.* **2012**, *48*, 7–10. [CrossRef]
57. Viegas-Junior, C.; Danuello, A.; da Silva Bolzani, V.; Barreiro, E.J.; Fraga, C.A.M. Molecular hybridization: A useful tool in the design of new drug prototypes. *Curr. Med. Chem.* **2007**, *14*, 1829–1852. [CrossRef]
58. Sashidhara, K.V.; Rao, K.B.; Kushwaha, P.; Modukuri, R.K.; Singh, P.; Soni, I.; Shukla, P.K.; Chopra, S.; Pasupuleti, M. Novel chalcone–thiazole hybrids as potent inhibitors of drug resistant Staphylococcus aureus. *ACS Med. Chem. Lett.* **2015**, *6*, 809–813. [CrossRef]
59. Sinha, S.; Manju, S.L.; Doble, M. Chalcone-Thiazole Hybrids: Rational Design, Synthesis, and Lead Identification against 5-Lipoxygenase. *ACS Med. Chem. Lett.* **2019**, *10*, 1415–1422. [CrossRef]
60. Shaik, A.; Shaik, M.S.; Puttagunta, S.B. (*E*)-1-(2′,4′-Dimethyl)-(5-acetylthiazole)-(2,4″-difluorophenyl)-prop-2-en-1-one. *Molbank* **2018**, *2018*, M1019. [CrossRef]
61. Kancharlapalli, V.R.; Shaikh, A.B.; Palleapati, K. Antitubercular evaluation of isoxazole appended 1-carboxamido-4,5-dihydro-1H-pyrazoles. *J. Res. Pharm.* **2019**, *23*, 156–163. [CrossRef]
62. Lokesh, B.V.S.; Prasad, Y.R.; Shaik, A.B. Synthesis, Biological evaluation and molecular docking studies of new pyrazolines as an antitubercular and cytotoxic agents. *Infect. Disord. Drug. Targets.* **2019**, *19*, 310–321. [CrossRef]
63. Lokesh, B.V.S.; Prasad, Y.R.; Shaik, A.B. Novel pyrimidine derivatives from 2,5-dichloro-3-acetylthienyl chalcones as antifungal, antitubercular and cytotoxic agents: Design, synthesis, biological activity and docking study. *Asian. J. Chem.* **2019**, *19*, 310–321. [CrossRef]
64. Shaikh, A.B.; Prasad, Y.R.; Shaik, S. Design, Facile Synthesis, Characterization and Computational Evaluation of Novel Isobutylchalcones as Cytotoxic Agents: Part-A. *FABAD J. Pharm. Sci.* **2015**, *40*, 7–22.
65. Shaik, A.B.; Prasad, Y.R.; Nissankararao, S.; Shahanaaz, S. Synthesis, Biological and Computational Evaluation of Novel 2, 3-dihydro-2-aryl-4-(4-isobutylphenyl)-1, 5-benzothiazepine Derivatives as Anticancer and Anti-EGFR Tyrosine Kinase Agents. *Anticancer. Agents. Med. Chem.* **2020**, *20*, 1115–1128. [CrossRef]
66. Kwofie, S.K.; Dankwa, B.; Odame, E.A.; Agamah, F.E.; Doe, L.; Teye, J.; Agyapong, O.; Miller, W.A.; Mosi, L.; Wilson, M.D. In silico screening of isocitrate lyase for novel anti-buruli ulcer natural products originating from Africa. *Molecules* **2018**, *23*, 1550. [CrossRef]
67. SwissADME. Available online: http://www.swissadme.ch/ (accessed on 24 March 2021).